

Documentation for the Global Human Modification of Terrestrial Systems

April 2020

C. M. Kennedy¹, J. R. Oakleaf², D. M. Theobald³, S. Baruch-Mordo⁴, and J. Kiesecker⁵

¹ Global Lands Program, The Nature Conservancy, Fort Collins, CO, 80524, USA

² Global Lands Program, The Nature Conservancy, Fort Collins, CO, 80524, USA

³ Conservation Science Partners, Fort Collins, CO, 80524, USA

⁴ Global Lands Program, The Nature Conservancy, Fort Collins, CO, 80524, USA

⁵ Global Lands Program, The Nature Conservancy, Fort Collins, CO, 80524, USA

Abstract

The Global Human Modification of Terrestrial Systems data set provides a cumulative measure of the human modification of terrestrial lands across the globe at a 1-km resolution. It is a continuous 0-1 metric that reflects the proportion of a landscape modified, based on modeling the physical extents of 13 anthropogenic stressors and their estimated impacts using spatially-explicit global data sets with a median year of 2016.

Data set citation: Kennedy, C. M., J. R. Oakleaf, D. M. Theobald, S. Baruch-Mordo, and J. Kiesecker. 2020. Global Human Modification of Terrestrial Systems. Palisades, NY: NASA Socioeconomic Data and Applications Center (SEDAC). <https://doi.org/10.7927/edbc-3z60>. Accessed DAY MONTH YEAR.

Suggested citation for this document: Kennedy, C. M., J. R. Oakleaf, D. M. Theobald, S. Baruch-Mordo, and J. Kiesecker. 2020. Documentation for the Global Human Modification of Terrestrial Systems. Palisades, NY: NASA Socioeconomic Data and Applications Center (SEDAC). <https://doi.org/10.7927/jw1p-am22>. Accessed DAY MONTH YEAR.

We appreciate feedback regarding this data set, such as suggestions, discovery of errors, difficulties in using the data, and format preferences. Please contact:

NASA Socioeconomic Data and Applications Center (SEDAC)
Center for International Earth Science Information Network (CIESIN)
Columbia University
Phone: 1 (845) 365-8920
Email: ciesin.info@ciesin.columbia.edu

Contents

I.	Introduction.....	2
II.	Data and Methodology.....	2
III.	Data Set Description(s).....	10
IV.	How to Use the Data.....	10
V.	Potential Use Cases.....	10
VI.	Limitations.....	11
VII.	Acknowledgments.....	12
VIII.	Disclaimer.....	13
IX.	Use Constraints.....	13
X.	Recommended Citation(s).....	13
XI.	Source Code.....	13
XII.	References.....	14
XIII.	Documentation Copyright and License.....	17
	Appendix 1. Data Revision History.....	17
	Appendix 2. Contributing Authors & Documentation Revision History.....	17

I. Introduction

The Global Human Modification (gHM) data set maps the degree of human modification on all terrestrial lands, excluding Antarctica, across the globe. gHM was derived from five major categories of stressors for which non-proprietary, spatial data existed globally on indicators (or proxies) at 1-km resolution: 1) human settlement (population density, built-up areas), 2) agriculture (cropland, livestock), 3) transportation (major roads, minor roads, two-tracks, and railroads), 4) mining and energy production (mining/industrial areas, oil wells and wind turbines), and 5) electrical infrastructure (powerlines and night-time lights). For each indicator, the most recent data was relied upon to capture contemporary land status with source years ranging from 2000-2016 and median and mean dates of 2016 and 2014, respectively.

II. Data and Methodology

In addition to this document, a detailed description of the methodology is available from:

- Kennedy, C. M., J. R. Oakleaf, D. M. Theobald, S. Baruch-Mordo, and J. Kiesecker. 2019. Managing the middle: A shift in conservation priorities based on the global human modification gradient. *Global Change Biology*. 25:811–826. <https://doi.org/10.1111/gcb.14549>.

Input data

Terrestrial lands were identified using the European Space Agency Climate Change Initiative (ESA CCI) land cover data set (European Space Agency, 2014), in which any 1 square kilometer (km²) cell with at least one 300m cell was labeled as terrestrial.

Table 1. Data input for gHM indicators of human modification

Stressor	Indicator	Name of Dataset	Data Feature	Resolution (Positional Accuracy)	Source Date	Source Citation
Human settlement	Human population density	Gridded Population of the World (GPW v4) – Pop Density Adjusted to 2015 UN	raster	1-km	2015	(Doxsey-Whitfield <i>et al.</i> , 2015)
	Built-up areas	Global Human Settlement Layer (GHSL)	raster	300m	2014	(Pesaresi <i>et al.</i> , 2013)
Agriculture	Cropland	Unified Cropland Layer	raster	250m	2014	(Waldner <i>et al.</i> , 2016)
	Livestock	Gridded Livestock of the World (GLWv2) – Cattle, Goats, Sheep	raster	1-km	2005	(Robinson <i>et al.</i> , 2014)
Transportation	Major roads	OpenStreetMap (OSM) – highway features (values: motorway, trunk, primary, and secondary)	lines	(± 20m)	2016	(OpenStreetMap Contributors, 2016)
	Minor roads	OSM – highway features (values: tertiary, unclassified, residential)	lines	(± 20m)	2016	(OpenStreetMap Contributors, 2016)
		gROADSv1		(± 500m)	1980-2010	(Center for International Earth

NASA Socioeconomic Data and Applications Center (SEDAC)
 Documentation for the Global Human Modification of Terrestrial Systems, v1 (2016)

Transportation						Science Information Network [CIESIN], Columbia University, and Information Technology Outreach Services [ITOS], University of Georgia, 2013)
	Two-tracks	OSM – highway features (values: tracks)	lines	(± 20m)	2016	(OpenStreetMap Contributors, 2016)
	Railroads	OSM – railway features (value: rail)	lines	(± 20m)	2016	(OpenStreetMap Contributors, 2016)
		Digital Chart of the World (DCW) – railroad features (value: operational)		(± 500m)	2000	(National Imagery and Mapping Agency, 1992)
Mining and energy production	Mining	OSM – land use features (values: industrial, quarry)	polygons	100m (± 20m)	2016	(OpenStreetMap Contributors, 2016)
	Oil wells	OSM – man-made features (value: petroleum_well)	points	(± 20m)	2016	(OpenStreetMap Contributors, 2016)
	Wind turbines	OSM – power features (values: generator, type: wind)	points	(± 20m)	2016	(OpenStreetMap Contributors, 2016)
Electrical infrastructure	Powerlines	OSM – power features (value: lines)	lines	(± 20m)	2016	(OpenStreetMap Contributors, 2016)
		DCW – utility features		(± 500m)	2000	(National Imagery and

		(value: power transmission line)				Mapping Agency, 1992)
Electrical infrastructure	Night-time lights	Defense Meteorological Satellite Program (DMSP) – Operational Linescan System (OLS v4) - Stable Lights	raster	1-km	2013	(Elvidge <i>et al.</i> , 2001)

Methods

The degree of HM was mapped based on three main steps. First, the spatial extent (H_e) for each indicator within a 1-km² pixel was estimated. To allow for cross comparison, all indicator values were rescaled between 0.00 (no modification) to 1.00 (high modification) based on the proportion of converted land for built-up areas, cropland, roads, powerlines, oil wells, wind turbines, mines or the $\log[X+1]$ transformed values for human population, livestock numbers, night-time lights (Table 2 and Table 3). H_e values were determined from empirical data (see *Indicator Method Descriptions by Stressor* below). Second, the degree of HM for each stressor indicator (HM_s) was calculated by multiplying its H_e by its potential magnitude of impact on natural terrestrial systems, referred to as intensity (H_i). Estimates of H_i were also scaled from 0.00 to 1.00 (see Table 3), and where possible, were based on a generalized land use coefficient that captured the per-unit amount of non-renewable energy required to maintain the human activity, termed Landscape Development Intensity (LDI) (Brown & Vivas, 2005). The uncertainty in H_i was accounted for by randomly selecting values from a uniform distribution (100 iterations) between a reported MIN and MAX range. Third, HM_s across stressor indicators were combined to derive a cumulative HM (HM_c) score using a fuzzy algebraic sum.

Accuracy Assessment

To assess the accuracy of mapped HM_c values, an independent validation data set on the degree of human modification based on visual interpretation of high-resolution aerial or satellite imagery for 1,000 plots (~1-km² “chips”) across the world was used. Plots were selected using the Global Grid sampling design (Theobald, 2016), which provided a spatially-balanced and probability-based random sampling across the global land extent (excluding Antarctica) that was stratified on a rural to urban gradient using “stable night-lights” 2013 imagery. Within each plot, 10 simple-random locations (for a total of 10,000 sub-plots) were selected, which were separated by a minimum distance of 100m and used to capture attributes for land cover class, land use class, dominant and secondary human stressor, and percent human modified following the Global Land Use Emergent Database (GLUED) protocol.

A strong agreement between average GLUED estimates and *HM* values were discovered. For the 989 ~1-km² plots analyzed, a strong correlation existed between these two measurements ($r = 0.78$ and $\rho = 0.77$), with an average error of approximately 14% (MAE = 14.18). Seven-hundred seven plots (71%) were within $\pm 20\%$ agreement between the mapped degree of *HMc* and the visual GLUED estimates. The remaining 212 plots (21%) had mapped *HMc* values greater than the GLUED estimates (false positive); and 70 plots (7%) had mapped *HMc* values less than the GLUED estimates (false negative). The main discrepancy can be attributed to *HMc* values tending to be higher than GLUED estimates (66% of total plots), particularly at high levels of development. Differences are primarily driven by human population densities, which cannot be directly observed from aerial images, and night-time lights, which can spillover to undeveloped areas, such as large parks and open spaces, from lit areas near or within major cities.

Table 2. Derived footprint values by indicator

Stressor	Indicator	<i>H_e</i> Input Values	<i>H_e</i> Output Values
Human settlement	Human population density	Pop density (PD): #people/km ²	Log (PD +1), max-normalized
	Built-up areas	Percent built-up: 0 (0%) – 255 (100%)	Proportion of 1-km ² cell
Agriculture	Cropland	Percent cropland	Proportion of 1-km ² cell
	Livestock	Livestock Density (LD): livestock units (LU)/km ²	Log (LU +1), max-normalized
Transportation	Major roads	Major road density/km ²	Proportion of 1-km ² cell using 0.030 km width
	Minor roads	Minor road density/km ²	Proportion of 1-km ² cell using 0.015 km width
	Two-tracks	Two-track road density/km ²	Proportion of 1-km ² cell using 0.003 km width

	Railroads	Railroad density/km ²	Proportion of 1-km ² cell using 0.010 km width
Mining and energy production	Mining	Industrial or quarry presence/absence	Proportion of 1-km ² cell
	Oil wells	Number of points/km ²	Proportion of 1-km ² cell using 0.014 km ² well pad size
	Wind turbines	Number of points/km ²	Proportion of 1-km ² cell using 0.0014 km ² wind turbine footprint
Electrical infrastructure	Powerlines	Powerline density/km ²	Proportion of 1-km ² cell using 0.015 km width
	Night-time lights	DN: 0 (min) to 63 (max brightness)	Log (DN + 1), max normalized

Table 3. Intensity value ranges by indicator

Stressor	Indicator	MIN H_i	MAX H_i
Human settlement	Human population density	0.20	0.50
	Built-up areas	0.69	1.00
Agriculture	Cropland	0.45	0.70
	Livestock	0.20	0.37
Transportation	Major roads	0.78	0.83
	Minor roads	0.39	0.50
	Two-tracks	0.10	0.20

	Railroads	0.78	0.83
Mining and energy production	Mining	0.83	1.00
	Oil wells	0.50	1.00
	Wind turbines	0.25	0.50
Electrical infrastructure	Powerlines	0.10	0.20
	Night-time lights	0.20	0.50

Indicator Method Descriptions by Stressor

Human settlement

Human settlement was mapped based on population density and the percentage of built-up areas. Because the distribution of population density using the GPW v4 was right-skewed (range: 0 – 732,202, median: 1.928), the top 0.1 percentile of cell values ($n = 135,415$) were collapsed, which fell at $> 4,246$ people/km², and then assigned this value to all top cells. These data were then $\log[X+1]$ transformed, producing values ranging from 0 to 3.628 (median: 0.467), which were then max-normalized. For built-up areas, the GHSL data were downscaled to 250m, and then the mean proportion of built-up within each 1-km² cell was calculated.

Agriculture

Agriculture was mapped based on cropland and livestock. For cropland, we calculated the mean proportion of cropland using the Unified Cropland Layer aggregating the 250m resolution cells to 1-km². For grazing, three data sets from Gridded Livestock of the World, Version 2 (GWLv2)--which identified the number of cattle, sheep, and goats--were used and converted to livestock units (LU) by multiplying the global average of livestock unit coefficients (cattle = 0.669, sheep = 0.104, and goats = 0.100) by the number of animals per km² (FAO, 2011). Values from these three data sets were summed to produce a total LU/km² (range: 0 – 1,391,520, median: 0.013). Cells with values $\geq 1,000$ LU/km² (10 LU/ha) ($n = 28,925$ cells, 0.01% of study extent) were collapsed and attributed the constant value of 1,000: a cutoff identified as a break-point between grazing and industrial livestock systems (Gerber *et al.*, 2010). Total LU/km² were $\log[X+1]$ transformed producing values ranging from 0 to 3.000 (median: 0.305), which were then max-normalized to 1.

Transportation

For transportation, major roads, minor roads, two-tracks, and railroads from OSM were used. Data-poor regions were augmented with the Global Roads Open Access Data Set,

Version 1 (gROADSv1) for road indicators, and with the Digital Chart of the World (DCW) vMap0 data (Danko, 1992) for the railway indicator. A single indicator of major roads was grouped from OSM highway features coded as either “motorway”, “trunk”, “primary”, or “secondary”. OSM features coded as “tertiary”, “unclassified”, and “residential” were categorized as minor roads, and augmented with gROADSv1 data. To avoid double counting, all OSM road data were buffered by 1-km and only gROADSv1 data occurring outside of the buffer were included. Finally, OSM features coded as “tracks” were used as the two-track indicator. For each road indicator, a linear road density (length in km/km²) was calculated for each 1-km² cell and multiplied by the typical road width associated with each road type: 0.030 km for major roads, 0.015 km for minor roads, and 0.003 km for two-tracks. The resulting total spatial extent was the proportion of a 1-km² cell composed of each road type indicator.

Similar methodologies were followed for railroads. All linear OSM features identified as railways were selected and augmented with DCW vMap0 railways that fell outside of a 1-km buffer. The linear density of railroads (i.e. length in km/km²) was calculated and multiplied by 0.010 km to calculate the total proportion of each of these indicators per 1-km² cell.

Mining and energy production

For mining and energy production, OSM data were used to calculate the proportion of each 1-km² cell containing mines, oil wells, or wind turbines. For mining, OSM land use features were used and selected polygons were identified as either “quarry” or “industrial” ($n = 441,623$), with the former identifying the mining pit and the latter the facility used for processing and shipping materials. The proportion of mining that overlapped each cell was then calculated.

For oil wells and wind turbines, OSM points were selected representing each of these indicators. The spatial extent of oil wells and wind turbines was calculated by summing the number of OSM wells and turbines mapped within each 1-km² cell, then multiplied by an estimated oil well pad size of 0.014 km² and wind turbine size of 0.0014 km². The result was the proportion of each energy production indicator per 1-km² cell.

Electrical infrastructure

Electrical infrastructure was based on above-ground powerlines and night-time lights. For powerlines, a methodology similar to the transportation indicators was applied. All linear OSM features identified as powerlines were selected and augmented with DCW vMap0 powerline features that fell outside of a 1-km buffer of the OSM powerlines. Linear density of powerlines was calculated and multiplied by a width of 0.015 km to derive the total proportion per 1-km² cell.

In an effort to capture any additional threats that were not included (natural gas wells) or were inadequately mapped by our indicator data sets (oil and gas wells and mining), the DMSP-OLS night-time lights (Elvidge *et al.*, 2001) was used, more specifically, the average visible, stable lights product for 2013. These data identify human presence through light intensity captured by satellite imagery and have digital number (DN) values

ranging from 0 (in areas where no lights are present) to 63 (in areas with high intensity of light throughout a year). The night-time lights values were $\log[X+1]$ transformed, resulting in a range from 0 to 1.806 (median: 0.929), which were then max-normalized.

III. Data Set Description(s)

Data set description:

The Global Human Modification of Terrestrial Systems data set provides a cumulative measure of the human modification of terrestrial lands across the globe at a 1-km resolution. It is a continuous 0-1 metric that reflects the proportion of a landscape modified, based on modeling the physical extents of 13 anthropogenic stressors and their estimated impacts using spatially-explicit global data sets with a median year of 2016.

Data set web page:

SEDAC URL:

<https://sedac.ciesin.columbia.edu/data/set/lulc-human-modification-terrestrial-systems>

Permanent URL: <https://doi.org/10.7927/edbc-3z60>

Data set format:

The Global Human Modification of Terrestrial Systems data set is available in two projections. The data were originally produced in Mollweide projection. The data has been reprojected in Geographic. Users should be aware that some spatial uncertainty is introduced in the re-projection process.

The data are available in GeoTIFF format in both Mollweide and Geographic projections as downloadable zip files. The downloadable is a compressed zip file, containing: 1) GeoTIFF, and 2) PDF documentation.

Data set downloads:

lulc-human-modification-terrestrial-systems-mollweide-geotiff.zip

lulc-human-modification-terrestrial-systems-geographic-geotiff.zip

IV. How to Use the Data

The raster data in GeoTIFF format can be used in any standard Geographic Information System (GIS) and software package for direct mapping and geospatial analysis.

V. Potential Use Cases

The Global Human Modification of Terrestrial Systems data set has many potential applications. The Nature Conservancy Global Development Risk Assessment (GDRA) suggests that these data can be used to address the challenges of land modification and

improve conservation strategies in landscape level mitigation, laws and regulations, lending requirements, and protection.

“The HM reveals that 95% of the Earth’s surface has some indication of human modification, and 84% has multiple human impacts. Most of the world is in a state of intermediate modification and fall within critical land use thresholds, with 52% of ecoregions and 48% of countries considered moderately modified. Given their vulnerability to further land change, moderately modified regions warrant conservation attention and require proactive spatial planning to maintain biodiversity and ecosystem function before environmental values are lost.” (<https://gdra-tnc.org/current/>)

See The Nature Conservancy Global Development Risk Assessment website for more information (<https://gdra-tnc.org>).

VI. Limitations

Despite its relative comprehensiveness, the *HM* map does not fully account for all human stressors. For example, it does not account for timber production, recreation, pastureland, pollution, and invasive species, which impact ecosystems (Salafsky *et al.*, 2008). Although spatial data may exist for these human stressors, these were not included due to data limitations, including incomplete global coverage or coarser mapping units (e.g., national or subnational scales) (Geldmann *et al.*, 2014, Kuemmerle *et al.*, 2013), or an inability to discern human-induced (timber harvesting or deforestation) from natural disturbances (natural fires, disease, storm damage) (Hansen *et al.*, 2013). Also, climate change was not included due to the uncertainty in the location and directionality of its impact on terrestrial systems (Geldmann *et al.*, 2014) and its diffuse nature, such that it’s unstoppable by localized human intervention (Tulloch *et al.*, 2015). Although some of the missing stressor indicators (invasive species, pollutants) are expected to be correlated with and may be captured by those included (Theobald, 2013), it is assumed that this assessment likely underestimates cumulative human stressors on terrestrial systems. This methodology, however, can be readily extended to include additional stressors and indicators as data and information become available.

Data derived from both remotely-sensed imagery and ground-based inventories were used. Included was data for human population and livestock densities (from global authoritative sources), as well as from citizen science efforts via online platforms like OSM (for energy production, extractive industry, road, rail, and electricity networks). As recently demonstrated for global roads (Ibisch *et al.*, 2016), crowd-sourced data like OSM enhance the spatial detail, accuracy, and attribution of human activities. It can also help validate land use maps and facilitate real-time monitoring of land use change (Fritz *et al.*, 2012). At the same time, such data sets have limitations and lack globally consistent coverage (as discussed in “Transportation” and “Mining and energy production” sections above); all of which can impose geographic biases, particularly in developing countries that often experience rapid land use change. That said, OSM road data have been shown to be ~83% complete and with >40% of countries deemed to have

fully-mapped street networks (Barrington-Leigh & Millard-Ball, 2017). Thus, crowd-sourced data remains valuable, especially for sectors like transportation, energy, and mining, which often have small, individual footprints that may be difficult to detect by satellite imagery, but cumulatively cause significant ecological impacts (Ibisch *et al.*, 2016, Raiter *et al.*, 2014). Our mapping efforts reinforce the need for improved global data coverage on land use activities less reliably captured from satellite imagery (i.e., energy, mining, grazing, and forestry activities) (Kuemmerle *et al.*, 2013) and volunteered geographic information plays a critical role (Fritz *et al.*, 2017).

For the H_i , intensity weightings were informed by energy-based indicators (Brown & Vivas, 2005), which offer a standardized measure of the levels of human-induced impacts on biological, chemical, and physical processes of surrounding lands from different human activities. While this metric has theoretical, empirical support for its use as a land use intensity metric (Brown & Ulgiati, 1997, Brown & Vivas, 2005), there are uncertainties and assumptions within its calculations (Hau & Bakshi, 2004). However, intensity values have been empirically verified in an ecological integrity assessment of U.S. landscapes (Theobald, 2013), and are in line with empirical syntheses on species responses to land use (Alkemade *et al.*, 2009, Benítez-López *et al.*, 2010, Newbold *et al.*, 2015). Yet, uncertainty still exists in the true magnitude of impacts from different human activities and how they vary across different ecosystems.

To derive HMc , it was assumed that the multiple effects of different stressors act cumulatively, but in a mitigative rather than an additive fashion. This minimized the bias of double-counting stressor data layers that are often non-mutually exclusive (Theobald, 2013), but also because it coincides with emerging evidence that stressor interactions may be more commonly non-additive than additive (Brown *et al.*, 2013, Crain *et al.*, 2008, Darling & Côté, 2008). As knowledge improves on how multiple human activities interact to affect ecosystems, our HM modelling approach can be updated accordingly.

VII. Acknowledgments

Funding for this research was provided by The Nature Conservancy, Anne Ray Charitable Trust, The 3M Foundation, and the NASA Land Cover Land Use Change Program.

Funding for dissemination of this data set was provided under the U.S. National Aeronautics and Space Administration (NASA) contract NNG13HQ04C for the continued operation of the Socioeconomic Data and Applications Center (SEDAC), which is operated by the Center for International Earth Science Information Network (CIESIN) of Columbia University.

VIII. Disclaimer

CIESIN follows procedures designed to ensure that data disseminated by CIESIN are of reasonable quality. If, despite these procedures, users encounter apparent errors or misstatements in the data, they should contact SEDAC User Services at ciesin.info@ciesin.columbia.edu. Neither CIESIN nor NASA verifies or guarantees the accuracy, reliability, or completeness of any data provided. CIESIN provides this data without warranty of any kind whatsoever, either expressed or implied. CIESIN shall not be liable for incidental, consequential, or special damages arising out of the use of any data provided by CIESIN.

IX. Use Constraints

This work is licensed under the Creative Commons Attribution 4.0 International License (<http://creativecommons.org/licenses/by/4.0>). 

Users are free to use, copy, distribute, transmit, and adapt the work for commercial and non-commercial purposes, without restriction, as long as clear attribution of the source is provided

X. Recommended Citation(s)

Data set(s):

Kennedy, C. M., J. R. Oakleaf, D. M. Theobald, S. Baruch-Mordo, and J. Kiesecker. 2020. Global Human Modification of Terrestrial Systems. Palisades, NY: NASA Socioeconomic Data and Applications Center (SEDAC). <https://doi.org/10.7927/edbc-3z60>. Accessed DAY MONTH YEAR.

Scientific publication:

Kennedy, C. M., J. R. Oakleaf, D. M. Theobald, S. Baruch-Mordo, and J. Kiesecker. 2019. Managing the middle: A shift in conservation priorities based on the global human modification gradient. *Global Change Biology*. 25:811–826. <https://doi.org/10.1111/gcb.14549>.

XI. Source Code

No source code is provided.

XII. References

- Alkemade R., van Oorschot M., Miles L., Nellemann C., Bakkenes M., and ten Brink B. 2009. GLOBIO3: a framework to investigate options for reducing global terrestrial biodiversity loss. *Ecosystems*, **12**, 374-390. <https://doi.org/10.1007/s10021-009-9229-5>.
- Benítez-López A., Alkemade R., and Verweij P. A. 2010. The impacts of roads and other infrastructure on mammal and bird populations: a meta-analysis. *Biological Conservation*, **143**, 1307-1316. <https://doi.org/10.1016/j.biocon.2010.02.009>.
- Brown C. J., Saunders M. I., Possingham H. P., and Richardson A. J. 2013. Managing for interactions between local and global stressors of ecosystems. *PLoS ONE*, **8**, e65765. <https://doi.org/10.1371/journal.pone.0065765>.
- Brown M. T., and Ulgiati S. 1997. Energy-based indices and ratios to evaluate sustainability: Monitoring economies and technology toward environmentally sound innovation. *Ecological Engineering*, **9**, 51-69. [https://doi.org/10.1016/S0925-8574\(97\)00033-5](https://doi.org/10.1016/S0925-8574(97)00033-5).
- Brown M. T., and Ulgiati S. 2002. Energy evaluations and environmental loading of electricity production systems. *Journal of Cleaner Production*, **10**, 321-334. [https://doi.org/10.1016/S0959-6526\(01\)00043-9](https://doi.org/10.1016/S0959-6526(01)00043-9).
- Brown M. T., and Vivas M.B. 2005. Landscape development intensity index. *Environmental Monitoring and Assessment*, **101**, 289-309. <https://doi.org/10.1007/s10661-005-0296-6>.
- Center for International Earth Science Information Network (CIESIN), Columbia University, and Information Technology Outreach Services (ITOS), University of Georgia. 2013. Global Roads Open Access Data Set, Version 1 (gROADSv1). Palisades, NY, NASA Socioeconomic Data and Applications Center (SEDAC). <https://doi.org/10.7927/H4VD6WCT>.
- Crain C. M., Kroeker K., and Halpern B. S. 2008. Interactive and cumulative effects of multiple human stressors in marine systems. *Ecology Letters*, **11**, 1304-1315. <https://doi.org/10.1111/j.1461-0248.2008.01253.x>.
- Danko D. M. 1992. The digital chart of the world project. *Photogrammetric Engineering and Remote Sensing*, **58**, 1125-1128.
- Darling E. S., and Côté I. M. 2008. Quantifying the evidence for ecological synergies. *Ecology Letters*, **11**, 1278-1286. <https://doi.org/10.1111/j.1461-0248.2008.01243.x>.
- Doxsey-Whitfield E., MacManus K., Adamo S. B., Pistolesi L., Squires J., Borkovska O., and Baptista S. R. 2015. Taking advantage of the improved availability of census data: A

first look at the Gridded Population of the World, version 4. *Papers in Applied Geography*, **1**, 226-234. <https://doi.org/10.1080/23754931.2015.1014272>.

Elvidge, C. D., Imhoff, M. L., and Baugh K. E. *et al.* 2001. Night-time lights of the world: 1994–1995. *ISPRS Journal of Photogrammetry and Remote Sensing*, **56**, 81-99. [http://doi.org/10.1016/S0924-2716\(01\)00040-5](http://doi.org/10.1016/S0924-2716(01)00040-5).

European Space Agency. 2014. Land Cover Map - 2010 epoch. Available at: <http://maps.elie.ucl.ac.be/CCI/viewer/>.

FAO. 2011. Guidelines for the preparation of livestock sector reviews. In: *Animal Production and Health Guidelines, No. 5*. pp 50, Rome, FAO.

Fritz S., McCallum I., and Schill C. *et al.* 2012. Geo-Wiki: An online platform for improving global land cover. *Environmental Modelling & Software*, **31**, 110-123. <https://doi.org/10.1016/j.envsoft.2011.11.015>.

Fritz S., See L., and Perger C. *et al.* 2017. A global dataset of crowdsourced land cover and land use reference data. *Scientific Data*, **4**, 170075. <https://doi.org/10.1038/sdata.2017.75>.

Gerber P., Mooney H. A., Dijkman J., Tarawali S., and De Haan C. 2010. *Livestock in a Changing Landscape, Volume 2: Experiences and Regional Perspectives*, Washington, D.C., Island Press.

Global Land Use Emergent Database Group. 2016. Global Land Use Emergent Database: A collaborative dataset on land use and land cover. <https://groups.google.com/forum/?fromgroups#!forum/global-land-use-emergent-database>.

Hansen M. C., Potapov P. V., and Moore R. *et al.* 2013. High-resolution global maps of 21st-century forest cover change. *Science*, **342**, 850-853. <https://doi.org/10.1126/science.1244693>.

Hau J. L., and Bakshi B. R. 2004. Promise and problems of energy analysis. *Ecological Modelling*, **178**, 215-225. <https://doi.org/10.1016/j.ecolmodel.2003.12.016>.

Ibisch P. L., Hoffmann M. T., and Kreft S. *et al.* 2016. A global map of roadless areas and their conservation status. *Science*, **354**, 1423-1427. <https://doi.org/10.1126/science.aaf7166>.

Kuemmerle T., Erb K., and Meyfroidt P. *et al.* 2013. Challenges and opportunities in mapping land use intensity globally. *Current Opinion in Environmental Sustainability*, **5**, 484-493. <https://doi.org/10.1016/j.cosust.2013.06.002>.

National Imagery and Mapping Agency. 1992. VMAP_1V10 - Vector Map Level 0 (Digital Chart of the World).

Newbold T., Hudson L. N., and Hill S. L. L. *et al.* 2015. Global effects of land use on local terrestrial biodiversity. *Nature*, **520**, 45-50. <https://doi.org/10.1038/nature14324>.

Dinerstein, E., Olson D., and Joshi A. *et al.* 2017. An ecoregion-based approach to protecting half the terrestrial realm. *Bioscience*, **67**, 534-545. <https://doi.org/10.1093/biosci/bix014>.

Openstreetmap Contributors. 2016. OpenStreetMap, the Free WikiWorld Map. Retrieved from www.openstreetmap.org.

Pesaresi M., Huadong G., and Blaes X. *et al.* 2013. A global human settlement layer from optical HR/VHR RS data: Concept and first results. *IEEE Journal of Selected Topics in Applied Earth Observations and Remote Sensing*, **6**, 2102-2131. <https://doi.org/10.1109/JSTARS.2013.2271445>.

Robinson T. P., Wint G. R. W., and Conchedda G. *et al.* 2014. Mapping the global distribution of livestock. *PLoS ONE*, **9**, e96084. <https://doi.org/10.1371/journal.pone.0096084>.

Salafsky N., Salzer D., and Stattersfield A. J. *et al.* 2008. A standard lexicon for biodiversity conservation: unified classifications of threats and actions. *Conservation Biology*, **22**, 897-911. <https://doi.org/10.1111/j.1523-1739.2008.00937.x>.

Theobald D. 2016. A General-Purpose Spatial Survey Design for Collaborative Science and Monitoring of Global Environmental Change: The Global Grid. *Remote Sensing*, **8**, 813. <https://doi.org/10.3390/rs8100813>.

Theobald D. M. 2010. Estimating natural landscape changes from 1992 to 2030 in the conterminous U.S. *Landscape Ecology*, **25**, 999-1011. <https://doi.org/10.1007/s10980-010-9484-z>.


Theobald D. M. 2013. A general model to quantify ecological integrity for landscape assessments and U.S. application. *Landscape Ecology*, **28**, 1859-1874. <https://doi.org/10.1007/s10980-013-9941-6>.

Theobald D. M., Zachmann L. J., Dickson B. G., Gray M. E., Albano C. M., Landau V., and Harrison-Atlas D. 2016. Description of the approach, data, and analytic methods used to estimate natural land loss in the western U.S. pp 23, *Conservation Science Partners*. <https://www.disappearingwest.org/>.

Tulloch V. J. D., Tulloch A. I. T., and Visconti P. *et al.* 2015. Why do we map threats? Linking threat mapping with actions to make better conservation decisions. *Frontiers in Ecology and the Environment*, **13**, 91-99. <https://doi.org/10.1890/140022>.

Waldner F., Fritz S., and Di Gregorio A. *et al.* 2016. A unified cropland layer at 250 m for global agriculture monitoring. *Data*, 1, 3. <https://doi.org/10.3390/data1010003>.

XIII. Documentation Copyright and License

Copyright © 2020. The Trustees of Columbia University in the City of New York. This document is licensed under a Creative Commons Attribution 4.0 International License (<http://creativecommons.org/licenses/by/4.0/>). 

Appendix 1. Data Revision History

No revisions have been made to this data set.

Appendix 2. Contributing Authors & Documentation Revision History

Revision Date	ORCID	Contributors	Revisions
April 29, 2020	0000-0002-9168-7172	James R. Oakleaf, Dara Mendeloff, Susana Adamo, Anne-Laure White	This document is the 1 st instance of documentation.